Using Artificial Neural Networks to Predict Impingement and Dislocation in Total Hip Arthroplasty

D. Alastruey-López[1], L. Ezquerra[2], B. Seral[1,2], M. A. Pérez[1*]

1. M2BE-Multiscale in Mechanical and Biological Engineering, Instituto de Investigación en Ingeniería de Aragón (I3A), Aragón Institute of Health Science (IACS), Universidad de Zaragoza, Campus Río Ebro, c/María de Luna s/n, 50018-Zaragoza, España {dalastruey@unizar.es; seralbelen@gmail.com; angeles@unizar.es}

2. University Clinic Hospital "Lozano Blesa", Aragón Institute of Health Science (IACS), University of Zaragoza,, Zaragoza, Spain {ezqlaura@gmail.com}

***Corresponding Author:**

Dr. Mª Ángeles Pérez Ansón

Mechanical Engineering, University of Zaragoza

Ed. Betancourt-Campus Río Ebro, C/María de Luna

50018 Zaragoza, Spain

Tel.: 00 34 876 55 52 13

E-mail: angeles@unizar.es

Abstract

Dislocation after total hip arthroplasty (THA) remains a major issue and an important post-surgical complication. Impingement and subsequent dislocation are influenced by the design (head size) and position (anteversion and abduction angles) of the acetabulum and different movements of the patient, with external extension and internal flexion the most critical movements. The aim of this study is to develop a computational tool based on a three-dimensional (3D) parametric finite element (FE) model and an artificial neural network (ANN) to assist clinicians in identifying the optimal prosthesis design and position of the acetabular cup to reduce the probability of impingement and dislocation. A 3D parametric model of a THA was used. The model parameters were the femoral head size and the acetabulum abduction and anteversion angles. Simulations run with this parametric model were used to train an ANN, which predicts the range of movement (ROM) before impingement and dislocation. This study recreates different configurations and obtains absolute errors lower than 5.5º between the ROM obtained from the FE simulations and the ANN predictions. The ROM is also predicted for patients who had already suffered dislocation after THA, and the computational predictions confirm the patient's dislocations. Summarizing, the combination of a 3D parametric FE model of a THA and an ANN is a useful computational tool to predict the ROM allowed for different designs of prosthesis heads.

Keywords: Artificial neural network, luxation prediction, parametric finite element, total hip arthroplasty

1. Introduction

Dislocation is a significant concern in total hip arthroplasty (THA) (Miki et al., 2013). Bozic et al. (2009) previously reported that instability had surpassed mechanical aseptic loosening as the most common cause of revision surgery. A patient who undergoes hip dislocations has reduced mobility, which directly affects the quality of life and increases the costs to the health system (Brown and Callaghan, 2008). Management of THA instability remains a surgical challenge and represents a multifactorial problem that includes the patient condition, surgical technique, implant component design and orientation, bone quality, and surrounding soft tissues (Brown and Callaghan, 2008; Barrack, 2003; Padgett and Warashina, 2004; Lawton and Morrey, 2004; Tanino et al, 2007; Kim et al., 2009; Fessy et al., 2017; Guo et al., 2017). Guo et al. (2017) remarked that many risk factors were identified for the dislocation following revision THA and that these factors were still undergoing controversial.

Many biomechanical studies based on the finite element (FE) method have evaluated the dislocation stability of different implant designs (Scifert et al., 1998; Nadzadi et al., 2003; Kluess et al., 2007; Elkins et al., 2011, 2012, 2015, Ezquerra et al., 2017; Terrier e al., 2017; Gao et al., 2018; Chi et al., 2018). All previous studies showed an added value with respect to a rigid body dynamics analysis. Elkins et al. (2012) performed a dynamic FE analysis to clarify the different consequences of bone-on-bone versus implant femoral neck and acetabular cup impingement (hardware impingement), and they concluded that bone-on-bone impingement was less prone to dislocation than hardware impingement. Large head diameters have been shown to prevent dislocation (Kluess et al., 2007; Ezquerra et al., 2017). Sciffert et al. (1998) described the relationship between range of movement (ROM)

and dislocation and showed that increasing the femoral head size increased the ROM. Terrier et al. (2017) performed a FE biomechanical analysis to compare a standard implant, a constraint implant and a dual mobility implant. Compared with the standard and constant implants, the dual mobility implants showed excellent performance in extending the ROM (Terrier et al., 2017; Gao et al., 2018). Several previous works established a "safe zone" with an optimal implant position and head size that reduced the risk of dislocation (Kluess et al., 2007; Elkins et al., 2015; Ezquerra et al., 2017;). Although, different reviews on this topic claimed that the establishment of a "safe zone" was not enough to prevent THA dislocation (Seagrave et al., 2017; Murphy et al., 2018; Tezuda et al., 2019).

Many different approaches can be tested using the FE method. Although FE analyses present the disadvantage of high computational cost, when a real-time response is required. The main objective of this work is to use a machine learning technique, artificial neural network (ANN) to rapidly and effectively predict the impingement and dislocation of THA. ANNs have been previously been used to predict atheroma plaque rupture (Cilla et al., 2012); femur (Garijo et al., 2014) and tibia (Garijo et al., 2017) loads; and damage accumulation in cancellous bone (Hambli, 2011). Therefore, the ultimate goal of this work is to develop a real-time computational tool to predict the ROM allowed after THA before impingement and dislocation. The tool will quantify the risk of dislocation for certain positions of the acetabular cup and for various designs of the prosthetic head. The methodology used to create this computational tool combines a 3D parametric FE model of the THA (Ezquerra et al. 2017) and a machine learning technique (ANN).

To the best of the authors' knowledge, this is the first publication focused on this type of analysis. A parametric tool based on machine learning techniques that is used to predict the ROM after THA has not been previously conducted. The tool may provide to the clinicians

with optimal prosthesis design and acetabular cup position to reduce post-op risk of dislocation. Additionally, the tool may allow to compare different position alternatives prior to the surgery process showing results of the suitability of each position considered by the surgeon.

2. Material and Methods

2.1 3D Parametric Finite Element Model

A parametric FE model of a hip prosthesis was previously developed (Ezquerra et al., 2017) to simulate impingement and dislocation for different femoral head sizes, acetabulum abduction (α) and anteversion (β) angles (Fig. 1). Impingement is the instant when the acetabulum and the femoral bone get in contact and the dislocation is produced when the femoral head gets out of its position inside the acetabulum.

The FE model was developed with Abaqus CAE v6.16 (Dassault Systèmes Simulia Corp., Suresnes, France) and consisted of two parts: the acetabulum and the femoral head and stem. The dimensions and geometry of the implant were obtained from a standard 37.5 mm-offset Exeter® cemented prosthesis (Stryker Ltd., Newbury, United Kingdom) with a collarless, smooth, polished and tapered stem (Choy et al., 2013). The acetabulum was modelled as a deformable solid with material properties that correspond to ultra-high-molecular-weight polyethylene (UHMWPE) (elastic modulus (E) of 940 MPa, Poisson's ratio of μ=0.3 and yield strength of 26.26 MPa to simulate the plastic properties of polyethylene) (Kluess et al., 2007; Ezquerra et al., 2017; Voigt et al., 2007). Due to the stiffness differences between the metal components of the femoral head and stem and the polyethylene of the acetabulum, the femoral head and stem were modelled as rigid parts

and their deformations were not considered. The mesh size was approximately 1.5 mm. A sensibility analysis was conducted by Ezquerra et al. (2017). Bone and soft tissue were not considered in the simulation.

A tangential isotropic contact model was defined between the femoral head and neck (master surfaces) and the inner hemisphere of the acetabulum component and the outer ring (slave surface). A friction coefficient of 0.038 was defined (Pedersen et al., 2005; Ezquerra et al., 2017).

Two types of movements were simulated until impingement and dislocation of the components occurred (Fig. 1): external extension (EE) and internal flexion (IF). EE corresponds to the standing position of the patient with an external rotation of the hip joint, whereas IF represents the seated position of the patient with an internal rotation of the hip joint (typical leg crossing manoeuvre) (Nadzadi et al., 2003).

The nodes of the external acetabulum component were fixed to simulate its complete fixation. All rotations were applied with respect to the reference point in the centre of the head (Fig. 1). The reader is referred to Ezquerra et al. (2017) for further details.

2.2 Source Data

Using the parametric FE model (section 2.1) different simulations were run. The inputs for each simulation were the femoral head sizes (22, 28, 32, 36 and 44 mm), acetabulum abduction angles (α) (20, 30, 40, 50, 60 and 70°) and acetabular anteversion angles (β) (0, 5, 10, 20, 30 and 40°) (Fig. 1). Therefore, 216 simulations were run for each type of movement (EE and IF). From each simulation, we obtained the maximum ROM allowed before impingement or dislocation.

2.3 Artificial Neural Network

ANNs are mathematical algorithms based on brain functioning that try to mimic the behaviour of the neurons (McCulloch and Pitts, 1943). A particular ANN is the multilayer perceptron (MLP). The main structure of the MLP includes an input layer, a hidden layer and an output layer (Fig. 2). Each one of these layers consists of a set of basic units called neurons.

ANNs also include a training algorithm that adjusts the weights and other parameters based on the input and output data provided to the network as well as the values that the network predicts (Fig. 2). A commonly used training algorithm in the MLP is the back-propagation algorithm (Bishop, 1995), which was chosen for training our network. The back-propagation algorithm uses supervised learning, which means that we provide the algorithm with examples of the inputs and outputs that we want the network to compute, and then the error (the difference between actual and expected results) is calculated. The main goal of the back-propagation algorithm is to minimize this error. The training begins with random weights, and the goal is to adjust them so that the error will be minimal.

The size of the input layer was determined by the number of input variables considered (Fig. 2). These input variables were the femoral head size, abduction angle (α) and anteversion angle (β) (section 2.2), which resulted in a three-neuron layer. The hidden layer was analysed and defined independently for each case. The output layer consisted of a single neuron that determined the maximum angle of the movement predicted, which is what delimits the ROM of the hip joint (section 2.2).

Several input connections along with the corresponding weights regulate the input signal intensities. An activation function that focuses on the input signals is needed. Additionally,

a transfer function should be chosen for the output of the neuron as a function of the input signals. ANNs can be configured with different transfer functions on each layer to generate their outputs. Laudani et al. (2015) performed a comprehensive review on the problem of choosing a suitable function for the hidden layer. Among the different transfer functions, the most usual transfer functions are logistic sigmoid (logsig), tangent sigmoid (tansig) and linear (purelin) (Fig. 3). These functions as well as *a* and *n* as the output and the input data, respectively, are explained below.

- The logistic sigmoid (logsig) generates an output between 0 and 1 according to equation 1, and input data range from negative to positive values.

$$a = \frac{1}{1+e^{-n}} \tag{1}$$

- The tangent sigmoid (tansig), which is an alternative to logsig in multilayer networks, generates an output between -1 and 1 (2).

$$a = \frac{e^{n}-e^{-n}}{e^{n}+e^{-n}} \tag{2}$$

- The linear transfer function (purelin) generates an output with a correlation of $a = n$.

A 10-fold cross-validation process was implemented to minimize the influence of the test set selection. In this paper, we randomly divided the data into two groups: 90% of the data were used to train the model and 10% of the data were used to test the model (Garijo et al., 2014).

Four independent ANNs were configured for impingement (i.e., the first collision between the acetabulum and femoral head/neck) and the dislocation (maximum ROM allowed) of the EE and IF movements. Different combinations of the previously defined transfer

functions were tested to find the optimal configuration for each ANN (section 2.4.1). The ANNs were implemented in MATLAB R2018b (MathWorks, Massachusetts, USA).

2.4 Method Performance and Validation

To choose the best ANN configurations (transfer functions-section 2.3) and then validate our proposed ANNs, different analyses were performed.

2.4.1 ANN performance and transfer function selection

The optimal configuration for each ANN was determined through an analysis of the performances of different transfer functions (Fig. 3) and a different number of neurons in the hidden layer (between 2 and 70 neurons) (Fig. 2). For this section, the results of the 216 simulations for each type of movement (EE and IF) (section 2.2) were used.

The configuration for each case was selected based on the absolute error (AE) (3), the correlation coefficient (RSQ) (4) and the time required to complete the training (Garijo et al., 2014). Five independent analyses were performed for each option. These repetitions ensure the stability of the selected configuration (standard deviation).

$$AE = ABS\left(\hat{\theta} - \theta\right) \tag{3}$$

$$RSQ = \frac{\sigma_{\hat{\theta}\theta}}{\sigma_{\hat{\theta}}\sigma_{\theta}} \tag{4}$$

Where $\hat{\theta}$ is the predicted ROM, θ is the real ROM, $\sigma_{\hat{\theta}\theta}$ is the covariance, and $\sigma_{\hat{\theta}}$ and σ_{θ} are the standard deviations. Results obtained for each configuration were summarized in section 3.1.

2.4.2 Validation 1: Parametric FE cases

Once the ANNs were configured, how accurate were ANN predictions compare with the values obtained in FE simulations was measured. From the work of Ezquerra et al. (2017), different combinations (23 cases) of femoral head sizes (28, 32 and 35 mm), acetabulum abduction angles (α) (25, 40 and 60°) and acetabular anteversion angles (β) (0, 15, 25°) were considered. These input value combinations were different from the source data (section 2.2) used to train the ANNs. Results obtained were summarized in Section 3.2.

Additionally, a paired sample T-test was performed for each analysed case to verify the ANN prediction with respect to the FE simulation results. The statistics (p-value and Pearson correlation coefficient) were calculated using the data analysis module in Excel (Microsoft Corporation, Washington, USA).

2.4.3 Validation 2: Patient-specific cases

After the computational validation with FE data, ANNs were also used to predict the ROM before impingement and dislocation in 5 patients who already had suffered hip dislocation after THA. The data for these 5 patients is shown in Table 1. The abduction and anteversion angles were measured from their corresponding computed tomography (CT) scans after the THA surgical procedure, where the position of the prosthesis was analysed.

3. Results

3.1 ANN performance and transfer function selection

Based on an analysis of the different possible combinations of transfer functions and the number of neurons in the hidden layer (section 2.4.1), the final configuration for each of the ANNs was established (Table 2). The time required for completing the training and testing

of each ANN is also indicated in Table 2. The absolute error of the selected combinations was lower than 6.5º, and the RSQ was close to 1 for all combinations. The mean time required for their training was less than 30 seconds.

3.2 Validation 1: Parametric FE cases

Results from the parametric FE model simulations (Ezquerra et al., 2017) and the ANN predictions (section 2.4.2) were detailed in Table 3. A summary was showed in Table 4. The mean error obtained for the ANNs was lower than 5.5º (Table 4), and the approximated maximum standard deviation was 5º.

The statistics show a significant difference ($p<0.05$ – Table 4) for both the impingement and luxation IF cases; nevertheless, considering the mean error and the standard deviation for these cases, the stability of the tool predictions can be assured (Table 4). The EE cases had a slightly higher standard deviation but significant differences were not observed ($p>0.05$), which implies a good correlation between the simulated ROM and the ANNs prediction.

3.3 Validation 2: Patient-specific Cases

Based on previously developed ANNs, the predicted ROMs for the 5 patients (Table 1) are presented in Table 5. Considering that all patients had already suffered hip prosthesis dislocation before the study development, the ROM limitation of each patient was determined by the lowest value obtained between the EE and IF results. Impingement of PS3 was predicted for an ROM of 33.74° and dislocation was predicted for an ROM of 43.64° under EE. PS1, 2, 4 and 5 predicted impingement and dislocation for IF (Table 5).

4. Discussion

The results show that using a 3D parametric FE model with an ANN represents a powerful tool for estimating the ROM after THA under different prosthesis designs (head size and acetabular cup orientation) and for different clinical manoeuvre.

The ANN performance AEs (for training and testing) were lower than 6.5º (Table 2). A comparison of the ANN estimations with the results of previous FE simulations (Ezquerra et al., 2017) showed that the calculated AEs were less than 5.5º (Table 3 and 4). Several experimental and clinical studies have analysed the ROM after THA under different manoeuvres. Kouyoumdjian et al. (2012) determined that the standard ROM for EE could be set to 37.9±8.4°. Our computational tool estimated that a ROM of 33.74° for PS3 was predictive of impingement, and this result could justify why PS3 suffered THA dislocation. A ROM of 37.9° was not observed (Kouyoumdjian et al., 2012). Nadzadi et al. (2003) determined that the standard ROM for IF could be set to approximately 50°. Therefore, our computational tool for the other patients (PS1, 2, 4 and 5) estimated an ROM lower than 50° for impingement and subsequent dislocation (see Table 5). These results justified the utility of the proposed computational tool.

In previous studies, Ezquerra et al. (2017) found a "safe zone" when the acetabulum component was placed at a 40-60° abduction angle and a 15-25° anteversion angle. These values were similar to those reported by Kluess et al. (2007) (45° abduction and 15-30° anteversion), Pedersen et al. (2005) (at least 40° abduction and 10° anteversion), Lewinneck et al. (1978) (40°±10 abduction and 15°±10 anteversion) ,Biedermann et al. (2005) (45°±10 abduction and 15°±10 anteversion) or Reina et al. (2017) (40-50° abduction and 15-30° anteversion). Fessy et al. (2017) found evidence that implanting the cup in 30°

to 50° inclination has a major impact on preventing dislocation. The position of the acetabulum component in the 5 patients analysed (Table 1) showed that the prosthesis was placed between the values of this predefined "safe zone" only in the case of PS1. Seagrave et al. (2017) performed a systematic reviewed to describe the different methods for measuring cup placement, target zones for cup positioning and the association between cup positioning and dislocation following primary THA. They concluded that the establishment of a safe zone based on the cup positioning and orientation was not enough to prevent THA dislocation (Seagrave et al., 2017; Murphy et al., 2018; Tezuda et al., 2019). Additionally, Tezuda et al. (2019) established that standard "safe zones" were outside the functional safe zone, identifying a potential reason hips dislocate despite leaving "safe zone" cup angles. Therefore, our computational tool could be a complementary tool to traditional "safe zone" theories. PS1 could be one of this "safe zone" failures.

The proposed computational tool based on an ANN trained and tested with data obtained from FE simulations has the potential for use in predicting the ROM in real patients with an error lower than 5.5º, which may help clinicians when identifying the most suitable position of the prosthesis prior to the surgical intervention. Easiness for ANNs training and low time required for obtaining results allow the revision of multiple options (design and cup orientations) with low computational cost, which could lead to a light implementation within minimum technical requirements.

Although the results obtained in this work were quite promising, the computational tool is based on several simplifications. The evaluation of more patient-specific cases could help to improve the accuracy of the tool and its validation. Additionally, acetabular polyethylene wear was not considered in the simulations, because instability created by prosthesis deterioration was not the main goal in this initial study but the direct consequences of the

movement that a patient can carry out. In the future, acetabular polyethylene wear could be simulated by incorporating a formulation based on the Archard wear law (Kruger et al., 2014). Elkins et al. (2015) incorporated in their simulations the capsule's contribution to THA stability. In our study, this factor was neglected. A parametric model that considers the capsule could be implemented and its parameters could be incorporated in the ANNs. Another limitation was the neglect of bone-on-bone impingement (Elkins et al., 2015), although impingement between the implant femoral neck and the acetabular cup remains the most common dislocation failure (Elkins et al., 2015). This study has not considered pelvic tilt factor, which relevance could be analysed and considered as a parameter for future developments of the predictive tool (Murphy et al., 2018; Hsu et al., 2019). Finally, the outer acetabulum component had a constant size (52 mm), and this consistency could be easily incorporated in a future parametric model and then into the computational tool based on the ANN.

Despite these limitations, the combination of a 3D parametric FE model of a THA and an ANN is a useful computational tool to predict the ROM allowed for different designs of prosthesis heads. Using these kind of methodologies, complex process can be simplified through ANNs configurations achieving low errors in the prediction. Clinically, the computational tool will allow the analysis of different alternatives for the prosthesis placement prior to the surgery. This methodology could be implemented in clinical practice to avoid time-consuming 3D FE analyses and it could be a complementary tool to well-defined "safe zones" previously established.

Acknowledgements

The authors would like to thank the Spanish Ministry of Economy and Competitiveness through project DPI 2014-53401-364-C2-1-R and DPI2017-84780-C2-1-R.

Conflict of interest

The authors of this manuscript declare that they have no financial and personal relationships with other people or organizations that could inappropriately influence their work.

References

1. Barrack R. L., 2003. Dislocation after total hip arthroplasty: implant design and orientation. J. Am. Acad. Orthop. Surg. 11: 89-99.
2. Biedermann R., Tonnin A., Krismer M., Rachbauer F., Eibl G., Stöckl B. 2005. Reducing the risk of dislocation after total hip arthroplasty. The effect of orientation of the acetabular component. J. Bone Joint Surg. Br. 87 (6): 762-769.
3. Bishop C. 1995. Neural networks and pattern recognition. Oxford University Press.
4. Bozic K. J., Kurtz S. M., Lau E., Ong K., Vail T. P., Berry D. J., 2009. The epidemiology of revision total hip arthroplasty in the United States. J. Bone Joint Surg. Am. 91(1): 128-133.
5. Brown T. D., Callaghan J. J., 2008. Impingement in total hip replacement: mechanisms and consequences, Curr. Orthop. 22: 376-391.
6. Chi W. M., Lin C. C., Ho Y. J., Lin J. C., Chen J. H. 2018. Using nonlinear finite element models to analyse stress distribution during subluxation and torque required

for dislocation of newly developed total hip structure after prosthetic impingement. Med. Biol. Eng. Comput. 56: 37-47.

7. Choy G. G., Roe J. A., Whitehouse S. L., Cashman K. S., Crawford R. W. 2013. Exeter short stems compared with standard length Exeter stems: Experience from the Australian Orthopaedic Association National Joint Replacement Registry. J Arthroplasty. 28 (1): 103–109.
8. Cilla M., Martínez J., Peña E., Martínez M. A. 2012. Atheroma Plaque Vulnerability Prediction using Machine Learning Techniques. IEEE Trans Biomed Eng. 59(4): 1155-1161.
9. Elkins J. M., Callaghan J. J., Brown T. D. 2015. The "landing zone" for wear and stability in total hip arthroplasty is smaller than we thought: a computational analysis. Clin. Orthop. Relat. Res. 473: 441-452.
10. Elkins J. M., Pedersen D. R., Callaghan J. J., Brown T. D. 2012. Bone-on-bone versus hardware impingement in total hips a biomechanical study. Iowa Orthop J. 32: 17-21.
11. Elkins J. M., Stroud N. J., Rudert M. J., Tochigi Y., Pedersen D. R., Ellis B. J., Callaghan J. J., Weiss J. A., Brown T. D. 2011. The capsule's contribution to total hip construct stability – a finite element analysis. J Orthop Res. 29 (11): 1642-1648.
12. Ezquerra L., Quilez M. P., Pérez M. A., Albareda J., Seral B. 2017. Range of Movement for Impingement and Dislocation Avoidance in Total Hip Replacement Predicted by Finite Element Model. J. Med. Biol. Eng. 37: 26-34.
13. Fessy M. H., Putman S., Viste A., Isida R., Ramdane N., Ferreira A., Leglise A., Rubens-Duval B., Bonin N., Bonnomet F., Combes A., Boisgard S., Mainard D., Leclercq S., Migaud H. 2017. What are the risk factors for dislocation in primary

total hip arthroplasty? A multicentre case-control study of 128 unstable and 438 stable hips. Orthop. Traumatol. Surg. Res. 103(5): 663-668.

14. Gao Y., Chen Z., Zhang Z., Chen S., Jin Z. 2018. Effect of inclination and anteversion angles on kinematics and contact mechanics of dual mobility hip implants. Clin. Biomech. 57: 48-55.
15. Garijo N., Martínez J., García-Aznar J. M., Pérez M. A. 2014. Computational evaluation of different numerical tools for the prediction of proximal femur loads from bone morphology. Comput. Methods Appl. Mech. Engrg. 268: 437–450.
16. Garijo N., Verdonschot N., Engelborghs K., García-Aznar J. M., Pérez M. A. 2017. Subject-specific musculoskeletal loading of the tibia: computational load estimation. J. Mech. Behav. Biomed. Mater. 65: 334-343.
17. Guo L., Yang Y., An B., Yang Y., Shi L., Han X., Gao S. 2017. Risk factors for dislocation after revision total hip arthroplasty: A systematic review and meta-analysis. Int. J. Surg. 38: 123-129.
18. Hambli R. 2011. Apparent damage accumulation in cancellous bone using neural networks. J. Mech. Behav. Biomed. Mater. 4(6): 868-878.
19. Hsu J., de la Fuente M., Radermacher K. 2019. Calculation of impingement-free combined cup and stem alignments based on the patient-specific pelvic tilt. J. Biomech. 82: 193-203.
20. Kim Y. H., Choi Y., Kim J. S. 2009. Influence of patient-, design-, and surgery-related factors on rate of dislocation after primary cementless total hip arthroplasty. J Arthroplasty. 24: 1258-1263.

21. Kluess D., Martin H., Mittelmeier W., Schmitz K. P., Bader R. 2007. Influence of femoral head size on impingement, dislocation and stress distribution in total hip replacement. Med. Eng. Phy. 29(4): 465–471.

22. Kouyoumdjian K., Coulomb R., Sánchez T., Asencio G. 2012. Clinical evaluation of hip joint rotation range of motion in adults. Orthop. Traumatol. Surg. Res. 98 (1): 17-23.

23. Kruger K. M., Tikekar N. M., Heiner A. D., Baer T. E., Lannutti J. J., Callaghan J. J., Brown T. D. 2014. A novel formulation for scratch-based wear modelling in total hip arthroplasty. Comput. Methods Biomech. Biomed. Engin. 17 (11): 1227-1236.

24. Laudani A., Lozito G. M., Riganti-Fulginei F., Salvini A. 2015. On training efficiency and computational costs of a feed forward neural network: A review. Comput. Intellig. Neurosc. 818243

25. Lawton R. L., Morrey B. F., 2004. Dislocation after long-necked total hip arthroplasty. Clin. Orthop. Relat. Res. 422: 164-166.

26. Lewinnek G. E., Lewis J. L., Tarr R., Compare C. L., Zimmerman J. R. 1978. Dislocation after total hip replacement arthroplasties. J. Bone Joint Surg. Am. 60: 217-220.

27. McCulloch W., Pitts W., 1943. A logical calculus of the ideas inmanent in nervous activity. Bulleting of Mathematical Biophysics. 5: 115-133.

28. Miki H., Sugano N., Yonenobu K., Tsuda K., Hattori M., Suzuki N., 2013. Detecting cause of dislocation after total hip arthroplasty by patient-specific four-dimensional motion analysis. Clin. Biomech. 28: 182-186.

29. Murphy W.S., Yun H., Hayden B., Kowal J.H., Murphy S.B. 2018. The safe zone range for cup anteversion is narrower than for inclination in THA. Clin. Orthop. Relat. Res. 476: 325-335.

30. Nadzadi M. E., Pedersen D. R., Yack H. J., Callaghan J. J., Brown T. D. 2003. Kinematics, kinetics, and finite element analysis of commonplace maneuvers at risk for total hip dislocation. J Biomech. 36: 577–591.

31. Padgett D. E., Lipman J., Robie B., Néstor B., 2006. Influence of total hip design on dislocation. Clin. Orthop. Relat. Res. 447: 48-52.

32. Padgett D. E., Warashina H. 2004. The unstable total hip replacement. Clin. Orthop. Relat. Res. 447: 60-65.

33. Pedersen D. R., Callaghan J. J., Brown T. D. 2005. Activity dependence of the ‘‘safe zone” for impingement versus dislocation avoidance, Med. Eng. Phy. 27 (4): 323–328.

34. Reina N., Putman S., Desmarchelier R., Sari Ali E., Chiron P., Ollivier M., Jenny J.Y., Waast D., Mabit C., de Thomasson E., Schwartz C., Oger P., Gayet L.E., Migaud H., Ramdane N., Fessy M. H. 2017. Can a target zone safer than Lewinnek’s safe zone be defined to prevent instability of total hip arthroplasties? Case-control study of 56 dislocated THA and 93 matched controls. Orthop. Traumatol. Surg. Res. 103: 657-661.

35. Scifert C. F., Brown T. D., Pedersen D. R., Callaghan J. J. 1998. A finite element analysis of factors influencing total hip dislocation. Clin. Orthop. Relat. Res. 355: 152-162.

36. Seagrave K.G., Troelsen A., Malchau H., Husted H., Gromov K. 2017. Acetabular cup position and risk of dislocation in primary total hip arthroplasty. A systematic review of the literature. Acta Orthop. 88(1): 10-17.

37. Tanino H., Harman M. K., Banks S. A., Hodge W. A. 2007. Association between dislocation, impingement, and articular geometry in retrieved acetabular polyethylene cups, Clin. Orthop. Relat. Res. 25: 1401-1407.

38. Terrier A., Latypova A., Guillemin M., Parvex V., Guyen O. 2017. Dual mobility cups provide biomechanical advantages in situations at risk for dislocation: a finite element analysis. Int. Orthop. 41: 551-556.

39. Tezuda T., Heckmann N. D., Bodner R. J., Dorr L. D. 2019. Functional safe zone is superior to the Lewinnek safe zone for total hip arthroplasty: why the Lewinnek safe zone is not always predictive of stability. J. Arthroplasty 34(1): 3-8.

40. Voigt C., Klöhn C., Bader R., von Salis-Soglio G., Scholz R. 2007. Finite element analysis of shear stresses at the implant-bone interface of an acetabular press-fit cup during impingement, Biomedizinische Technik. 52 (2): 208–215.

LIST OF FIGURES

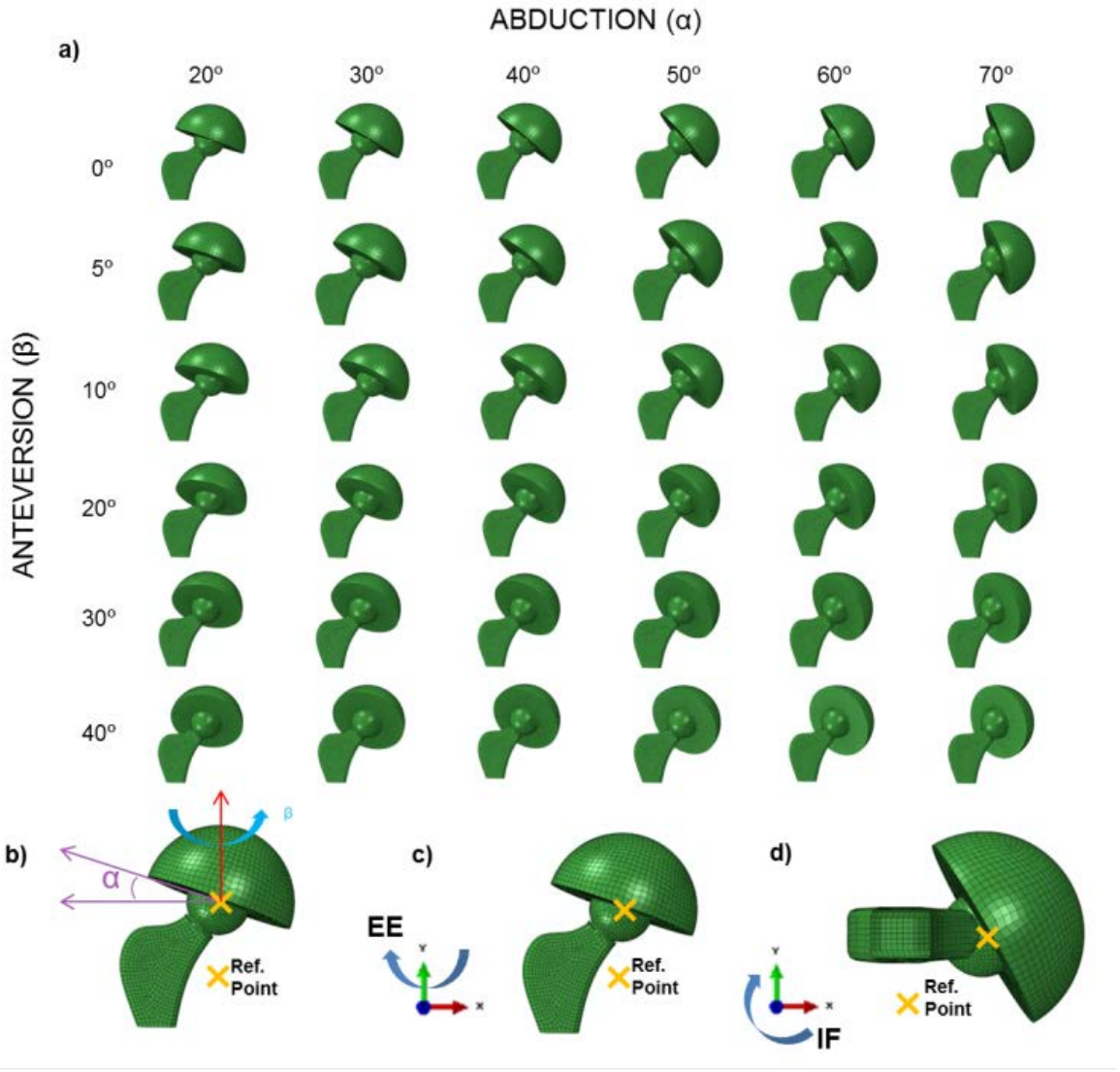

Figure 1. a) Positions considered in the FE analysis to obtain the training data, b) reference angles, c) external extension (EE) rotation, and d) internal flexion (IF) rotation.

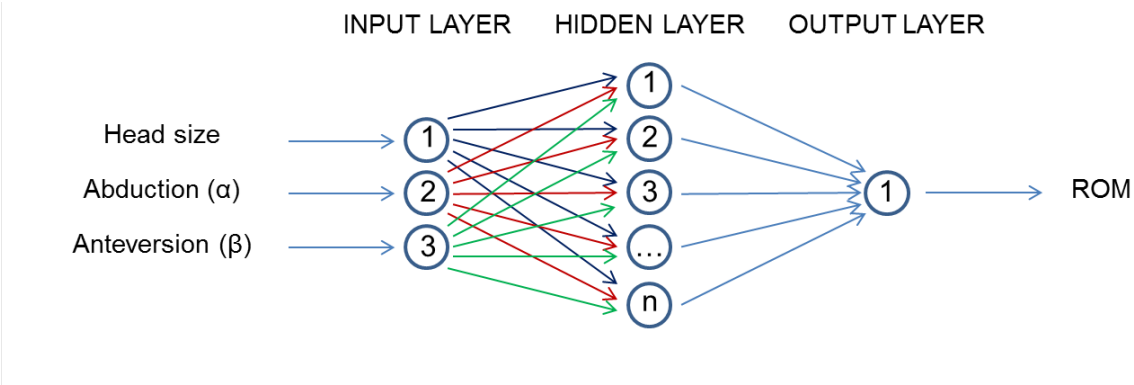

Figure 2. General structure of the ANNs considered in the study.

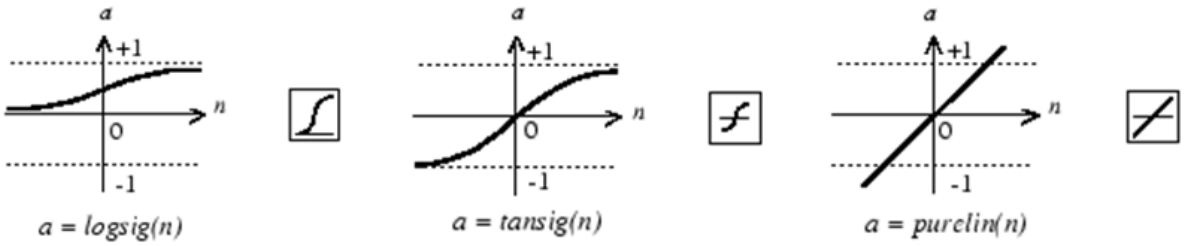

Figure 3. Main transfer functions considered in the study for the ANN configuration (MathWorks, Massachusetts, USA).

LIST OF TABLES

Table 1. Patient-Specific data included for the ANN final validation. F=Female; M=Male; α=abduction angle; β=anteversion angle.

Patient	Age (yr)	Gender	Weight (kg)	Head Size (mm)	α (°)	β (°)
PS1	86	M	70	28	46,69	18,99
PS2	91	F	60	28	38,8	20,81
PS3	66	F	86	32	62	42
PS4	72	F	95	32	31,77	22
PS5	80	M	96	32	48,59	0

Table 2. Summary of the absolute error (AE) and the correlation coefficient (RSQ) of the different ANNs (EE=External extension; IF=Internal flexion; Imp=Impingement; Dis=Dislocation; and σ=Standard deviation).

Case	EE Imp	EE Dis	IF Imp	IF Dis
Hidden Layer Transfer Function	tansig	logsig	tansig	tansig
Hidden Layer Neurons	3	8	7	9
OL Transfer Function	logsig	purelin	purelin	tansig
AE (°)	4,57	6,12	3,67	4,41
σ (AE) (º)	4,733	6,043	2,907	2,576
RSQ	0,930	0,823	0,946	0,900
σ (RSQ)	0,043	0,101	0,031	0,031
Time (s)	8,69	25,61	24,70	26,89
σ (Time)	0,66	1,23	1,33	3,46

Table 3. Results Obtained for the 23 Finite Element Simulated Validation Cases. α=Abduction angle; β=Anteversion angle; AE=Absolute error; σ=Standard deviation; EE=External extension; IF=Internal flexion; Imp=Impingement; and Dis=Dislocation.

				EE Imp			EE Dis			IF Imp			IF Dis		
Case	Head Size (mm)	α (º)	β (º)	Real ROM (º)	Pred. ROM (º)	AE (º)	Real ROM (º)	Pred. ROM (º)	AE (º)	Real ROM (º)	Pred. ROM (º)	AE (º)	Real ROM (º)	Pred. ROM (º)	AE (º)
1	28	60	25	86,40	77,80	8,60	92,45	96,38	3,93	18,00	22,90	4,90	54,00	61,59	7,59
2	28	25	0	61,20	62,15	0,95	96,21	103,51	7,30	19,80	28,04	8,24	0,00	1,70	1,70
3	36	25	25	93,60	81,48	12,12	78,70	64,22	14,47	0,00	1,52	1,52	21,78	26,81	5,03
4	28	25	15	54,00	56,33	2,33	77,94	75,75	2,19	0,00	0,00	0,00	24,34	17,44	6,89
5	28	25	25	145,12	152,67	7,56	62,66	62,93	0,27	37,80	42,10	4,30	26,57	25,18	1,39
6	28	40	25	86,40	85,67	0,73	91,71	83,27	8,44	41,40	45,83	4,43	35,78	40,88	5,09
7	36	40	15	100,80	100,64	0,16	97,27	103,18	5,90	9,00	8,93	0,07	30,60	34,80	4,20
8	36	25	15	59,85	63,89	4,04	97,27	83,09	14,18	0,00	0,00	0,00	23,42	19,63	3,79
9	36	25	0	96,21	92,88	3,33	76,43	76,46	0,03	45,00	48,36	3,36	0,00	3,85	3,85
10	32	60	25	64,80	66,63	1,83	94,63	84,52	10,10	3,60	11,32	7,72	53,96	62,63	8,67
11	32	25	0	70,20	67,04	3,16	68,51	68,52	0,02	44,33	54,58	10,25	0,00	4,01	4,01
12	36	40	25	68,40	68,05	0,35	65,63	64,56	1,07	12,60	19,20	6,60	36,00	42,18	6,18
13	32	40	15	73,13	70,14	2,99	128,72	148,06	19,34	30,60	32,13	1,53	33,28	34,93	1,64
14	36	60	25	77,40	78,79	1,39	113,67	115,70	2,03	9,00	8,64	0,36	59,74	62,16	2,41
15	28	60	15	81,00	73,95	7,05	101,90	103,96	2,06	18,00	15,95	2,05	48,11	54,04	5,93
16	28	45	0	54,00	53,89	0,11	74,09	69,08	5,01	3,60	5,72	2,12	25,34	22,27	3,07
17	32	25	25	128,72	143,12	14,40	69,03	75,01	5,98	30,60	35,64	5,04	25,96	26,69	0,73
18	32	60	15	54,00	50,82	3,18	145,12	149,05	3,93	21,60	26,16	4,56	51,39	55,42	4,03
19	32	40	25	59,40	62,54	3,14	145,35	141,16	4,19	18,00	12,59	5,41	38,93	42,26	3,33
20	36	60	15	57,94	56,99	0,96	61,02	63,78	2,76	55,80	57,34	1,54	51,53	54,85	3,32
21	28	40	15	68,40	58,35	10,05	64,30	61,95	2,35	14,40	18,91	4,51	35,69	33,09	2,60
22	28	35	0	117,00	132,77	15,77	65,70	66,37	0,67	0,00	0,00	0,00	0,00	11,83	11,83
23	32	25	15	91,80	92,18	0,38	69,32	66,48	2,83	45,00	50,83	5,83	23,58	19,49	4,09
Mean AE						4,55			5,18			3,67			4,41
σ						4,71			5,11			2,91			2,58

Table 4. Summary of the results and statistics obtained for the 1st validation with 23 computational cases (EE=External extension; IF=Internal flexion; Imp=Impingement; Dis=Dislocation; and σ=Standard deviation).

Case	Mean AE (º)	σ (AE) (º)	p-value	Pearson Correlation Coefficient
EE Imp	4,547	4,714	0,9750	0,9770
EE Dis	5,177	5,112	0,7665	0,9661
IF Imp	3,667	2,906	0,0007	0,9834
IF Dis	4,408	2,576	0,0141	0,9726

Table 5. Predicted ROM for each patient-specific analysis. Luxation is observed in external extension for patient 3 and in internal flexion for the other 4 cases (EE=External extension; IF=Internal flexion; Imp=Impingement; and Dis=Dislocation).

	EE Imp	EE Dis	IF Imp	IF Dis
Patient	Angle (º)	Angle (º)	Angle (º)	Angle (º)
PS1	65,71	74,44	30,30	43,54
PS2	65,18	72,35	22,97	36,65
PS3	33,74	43,64	65,89	71,23
PS4	68,25	73,42	20,40	31,79
PS5	92,91	100,09	15,38	27,89